IEEE Access
Multidisciplinary ⋮ Rapid Review ⋮ Open Access Journal

Received May 13, 2022, accepted May 29, 2022, date of publication June 17, 2022, date of current version June 23, 2022.

Digital Object Identifier 10.1109/ACCESS.2022.3184020

A K/Ka-Band Reconfigurable Substrate Integrated Coaxial Line to Waveguide Transition Technology

YIFANG WEI[1], (Graduate Student Member, IEEE), CHRISTIAN ARNOLD[2], AND JIASHENG HONG[1], (Fellow, IEEE)

[1]School of Engineering and Physical Sciences, Heriot-Watt University, Edinburgh EH14 4AS, U.K.
[2]Tesat-Spacecom GmbH & Co. KG Backnang, 71522 Backnang, Germany

Corresponding author: Yifang Wei (y.wei@hw.ac.uk)

The work of Yifang Wei was supported by the European Union's Horizon 2020 Research and Innovation Program under the Marie Skłodowska-Curie Grant through the Advanced Technologies for future European Satellite Applications (TESLA) Project under Grant 811232.

ABSTRACT In this article, the designs of the K/Ka-Band reconfigurable Substrate Integrated Coaxial Line (SICL)-to-waveguide transitions are presented. Two types of reconfigurable SICL-to-waveguide transitions, with stepped impedance transformers waveguide transitions and ridge waveguide transitions, are designed for two operation frequency modes (K/Ka-band). Both simulated and experimental results are presented for the demonstration. Results indicate that the reconfigurable waveguide structure has the advantages of broad bandwidth and low return loss for both K/Ka-band compared with the conventional dual-band waveguide transitions. The presented waveguide transition designs with high function flexibility will be significant to satellite communication applications and massive MIMO beamforming networks with an active phased antenna array.

INDEX TERMS SICL-to-waveguide transition, dual-band, satellite communication, multilayer MIMO beamforming.

I. INTRODUCTION

In modern satellite communications beamforming technologies, the beamforming system needs dual-band operation frequencies for separate uplink and downlink to reduce the influence and interference [1]. In other words, the transmission (Tx) and reception (Rx) systems are usually frequency separated to achieve a better downlink margin [2].

Due to the wider bandwidth requirement for higher frequency designs, the high-frequency transmission line structures developed rapidly in recent years. The Substrate Integrated Coaxial Line (SICL) structure has the advantages of compact footprint, wide bandwidth, low loss, and interference in high-frequency applications [3]. It is also applicable in a multilayer PCB feeding network, which is promising for reducing the size of the feeding network and increasing the design diversity and flexibility in a MIMO beamforming system. Compared with the coaxial interconnections and transitions to the phased antenna array in a beamforming system, the waveguide transitions have merits in their simple installation and maintenance, which are also popular in RF communication applications for their low loss, wideband performance, and simple structure [4]–[11]. Therefore, SICL-to-waveguide transition designs have great potential for a multilayer MIMO beamforming technology to achieve more flexible functions, especially in satellite communication applications.

Microstrip-to-waveguide transitions were designed with good insertion loss and compact structure [4]–[9]. To be more applicable for a high-frequency multilayer network, SICL-to-waveguide and Substrate Integrated Suspended Line (SISL)-to-waveguide transition designs demonstrated their wideband performance and low loss [10], [11]. However, they are all focused on a single-band operation. Dual-band designs to achieve dual K/Ka-band operation performance in a satellite communication system were presented recently [12]–[14]. They commonly sacrifice bandwidth and performance to achieve dual-band operations. Furthermore, some dual-band waveguide transition designs have operation frequency range limitations [13].

Therefore, the motivation for this work is to develop waveguide transitions at K/Ka-band (20 GHz/30 GHz).

The associate editor coordinating the review of this manuscript and approving it for publication was Mohammad Zia Ur Rahman.

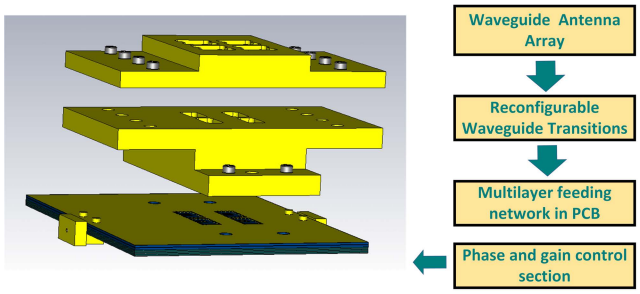

FIGURE 1. Beamforming system network.

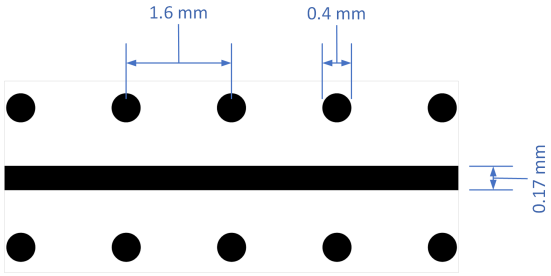

FIGURE 2. SICL structure with dimensions.

For this purpose, the two types of reconfigurable SICL-to-waveguide vertical transitions with two operation frequency modes (K/Ka-band) were developed. They provide promising solutions to achieve better wideband performance for the K/Ka-band separated Rx and Tx, which traditionally have two different systems for Rx and Tx with different dimensions. These two types of reconfigurable SICL-to-waveguide transitions have the same waveguide dimension for the same operation mode. Furthermore, the two K/Ka-band mode waveguides share the same SICL PCB feeding network in beamforming applications. Only metallic waveguide parts need to be replaced to achieve K/Ka-band (Tx/Rx) operation modes switching, saving cost, simplifying installation and maintenance, and providing flexible functions.

II. DESIGN OF THE SICL-TO-WAVEGUIDE TRANSITION

In a beamforming system, the SICL-to-waveguide transition connects the feeding network in PCB and the waveguide antenna array. An example of a 2 × 2 beamforming antenna array is illustrated in Fig. 1 to show the beamforming system network. The phase and gain control section would be installed at the bottom of the multilayer PCB feeding network.

A. RECTANGULAR WAVEGUIDE TRANSITIONS WITH STEPPED TRANSFORMERS

The SICL structure, shown in Fig. 2, provides low loss and wideband performance for a high-frequency multilayer PCB feeding network in a beamforming system. Its two side rows of metallic vias reduce resonance interference in the beamforming feeding network in a compact structure [3].

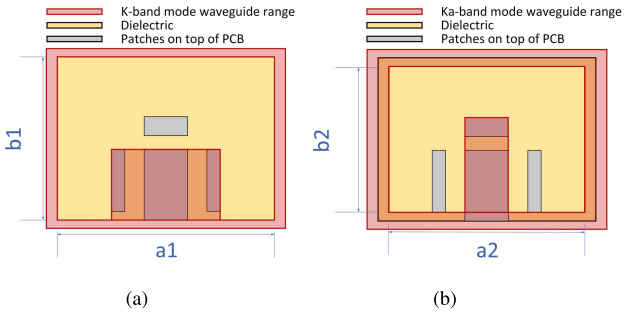

FIGURE 3. Concept of two modes switched for the SICL-to-waveguide transitions for (a) K-band mode and (b) Ka-band mode. The dimensions are a1 = 9, b1 = 4.5, a2 = 8.5, b2 = 4.25, all in millimeters.

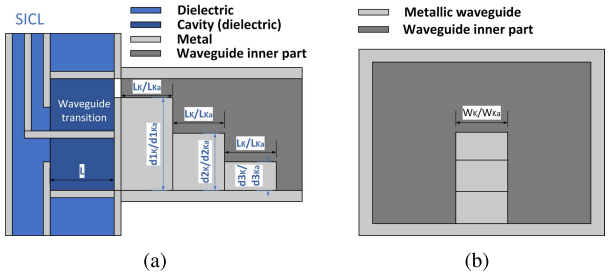

FIGURE 4. (a) Side view and (b) top view of the rectangular SICL-to-waveguide transition with stepped transformers. The dimensions are L = 11, WK = 28, WKa = 12, d1K = 26.5, d1Ka = 29, LK = 37, LKa = 21, all in millimeters.

The adaptable patches on top of the PCB could help match the impedance for the two modes and reduce the interference between them to achieve dual-mode operations at K/Ka-band, shown in Fig. 3 (a) and (b). Contrary to the conventional designs, the two modes for K/Ka-Band share the same PCB feeding network. The waveguide parts with two different dimensions for K/Ka-band connect to the same PCB. They can be installed and replaced easily (screws), as demonstrated in Fig. 1, to achieve different modes of operation at different frequencies.

The stepped transformers are adopted in this waveguide transition design to increase the impedance from SICL to the waveguide and convert the propagation mode from quasi-TEM in a SICL to TE10 in a waveguide [15]. The side view and top view of the rectangular SICL-to-waveguide transition with stepped transformers are illustrated in Fig.4 (a) and (b), and the E-field distributions are shown in Fig. 5 (a) and (b).

To meet the requirements in a beamforming system to provide a better antenna elements distance for better performance at K/Ka-band, there is a dimension limitation of 10 mm for every element. Therefore, the broad wall width of the K-band and Ka-band modes waveguides in this design are 9 mm and 8.5 mm, respectively. When the broad wall is 9 mm, the cut-off frequency is around 16.7 GHz, and the waveguide still works in the required frequency range for K-band. The narrow wall width is around half of the broad wall width.

The SICL structure and the waveguide are connected by a via, whose equivalent circuit model is shown in Fig. 6 (a) [16].

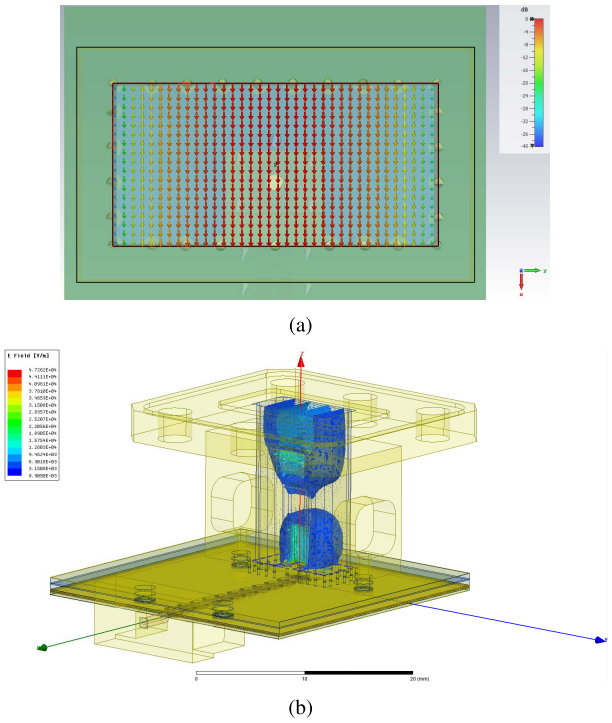

FIGURE 5. E-field distributions of (a) the waveguide port and (b) the waveguide part in the SICL-to-waveguide transition with stepped transformers.

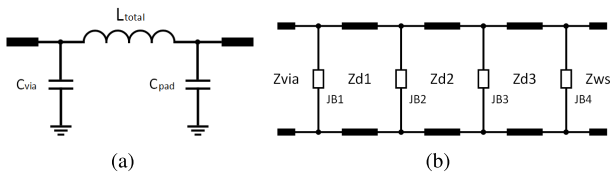

FIGURE 6. Equivalent circuit models of (a) Via and (b) stepped transformers.

The stepped transformers from via (Zvia) to waveguide (Zws) could be represented by the equivalent circuit model shown in Fig. 6 (b) [17]. The reactive energy of the fringing fields at each waveguide step is represented by susceptances B1, B2, B3 and B4. The Zd1, Zd2 and Zd3 represent the impedances of stepped transformers.

The simulation results in Fig. 7 (a) and (b) show the wideband performance for K/Ka-band operation modes with the bandwidth of 36.6% (18.1 GHz - 26.2 GHz) and 38.1% (21.7 GHz - 31.9 GHz) for return loss better than 10 dB, respectively.

B. RIDGE WAVEGUIDE TRANSITIONS

The reconfigurable ridge waveguide transitions have a similar design to the waveguide transitions with stepped transformers to achieve K/Ka-band dual-mode operation by using the adaptable patches on top of the PCB. The identical waveguide dimensions and adaptable patches make these two types of SICL-to-waveguide transitions match the same PCB feeding

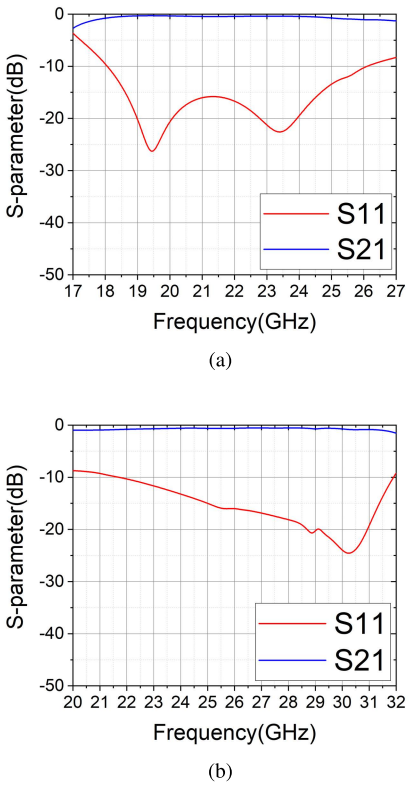

FIGURE 7. Simulated results of waveguide transitions with stepped transformers for (a) K-band mode and (b) Ka-band mode.

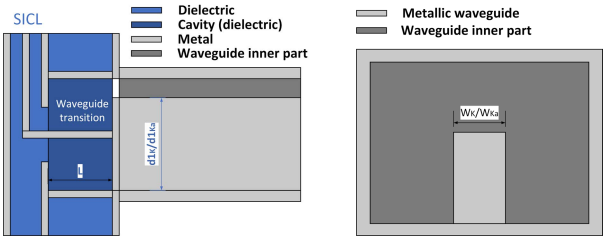

FIGURE 8. (a) Side view and (b) top view of the ridge SICL-to-waveguide transition. The dimensions are L = 11, WK = 28, WKa = 12, d1K = 26.5, d1Ka = 29, all in millimeters.

network in a beamforming system for the same operation mode.

The ridge waveguide structure is adopted in this design to get a broader bandwidth performance [18], [19]. The loss of waveguide transitions with stepped transformers for K-band mode below 18 GHz increases due to its cut-off frequency being around 16.7 GHz. The ridge waveguide structure provides a lower TE10 cut-off frequency for better bandwidth performance for the same broad wall width to meet the requirements for a beamforming system.

The side view and top view of the ridge structure SICL-to- waveguide transition are illustrated in Fig. 8 (a) and (b), and the E-field distributions are shown in Fig. 9 (a) and (b).

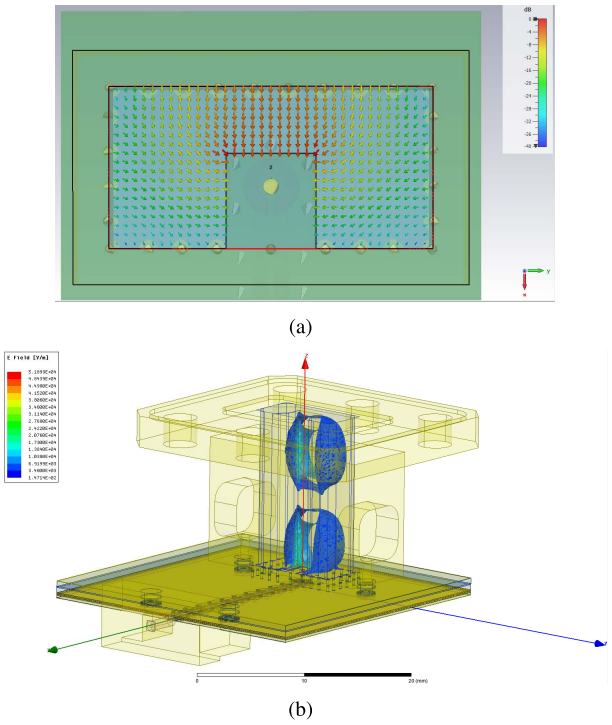

FIGURE 9. E-field distributions of (a) the waveguide port and (b) the waveguide part in the ridge SICL-to-waveguide transition.

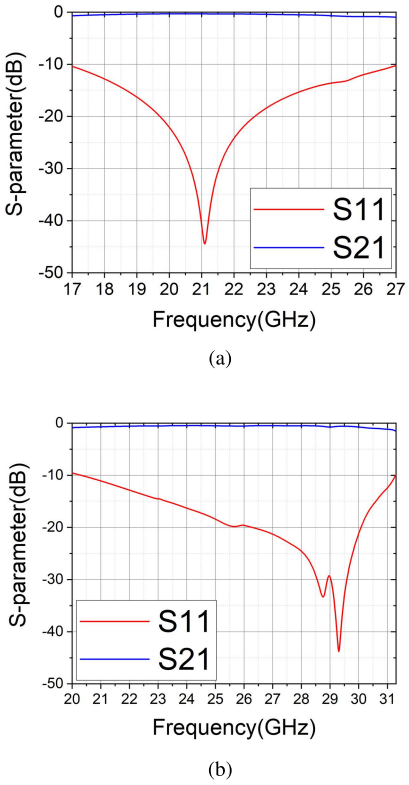

FIGURE 10. Simulated results of ridge waveguide transitions for (a) K-band mode and (b) Ka-band mode.

The ridge SICL-to-waveguide transitions simulation results are shown in Figs. 10 (a) and (b). They demonstrate wider bandwidth performance for both K/Ka-band operation

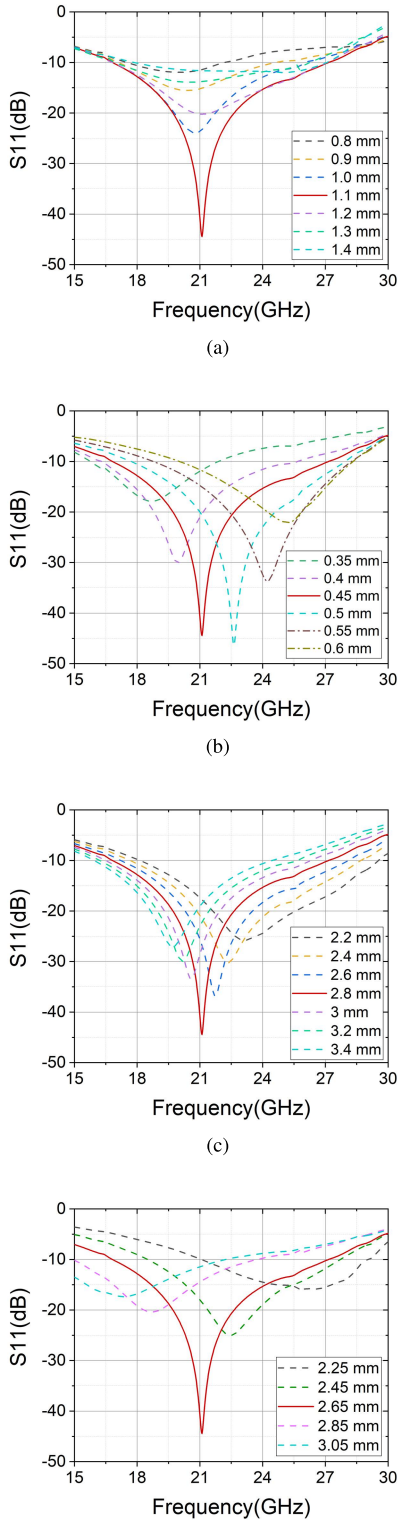

FIGURE 11. Simulated reflection coefficients for different parameters. (a) Various values of cavity height L, (b) various values of via diameter Dv, (c) various values of stepped transformer width W and (d) various values of ridge depth d1.

modes with a bandwidth of 50.5% (16.3 GHz - 27.3 GHz) and 43.7% (20.4 GHz - 31.8 GHz) for return loss better than

(a) (b)

FIGURE 12. (a) Fabricated SICL-to-waveguide transitions and (b) the back-to-back structure in the measurement.

10 dB, respectively, compared with the SICL-to- waveguide transition with stepped transformers.

In a beamforming application, adding an 8.5 mm × 4.25 mm to 9 mm × 4.5 mm waveguide transition to the K-band mode waveguide port does not significantly influence the performance and helps the two modes designs have the same waveguide dimension on both K/Ka-band. Therefore, the two K/Ka-band waveguides could connect and feed the same wideband waveguide antenna array in a beamforming system with separated Rx and Tx, improving flexibility and cost-efficiency and simplifying installation.

The cavity height L, via diameter Dv, ridge depth d1 and stepped transformer width W are critical to these two SICL-to-waveguide transition designs. The analysis in Figs. 11 (a), (b), (c), and (d) demonstrates the effects of these transition parameters on the K-band mode ridge SICL-to-waveguide transition. The cavity height L is critical for the propagation mode transformation from a SICL to a waveguide. The via diameter Dv and width W of the ridge (or the stepped transformers) significantly influences the operation frequency range. The operation range moves to a higher frequency when the via diameter Dv increases or the ridge width W decreases. The ridge depth d1 helps the impedance matching to get better performance.

III. EXPERIMENT RESULTS

A grounded coplanar waveguide (GCPW) structure was deployed and extended from the SICL to the edge of the test ports on a K-connector to facilitate experimental testing of the two kinds of designed SICL-to-waveguide vertical transitions. The fabricated SICL-to-waveguide transition is shown in Fig. 12 (a). The back-to-back structure was used in the measurement, shown in Fig. 12 (b). The measured and simulated results of the SICL-to-waveguide transition with stepped transformers and the ridge SICL-to-waveguide transition are shown in Figs. 13 (a) and (b) and Figs. 13 (c) and (d), respectively. The measured insertion loss and return loss results agree relatively well with the simulations (including the connectors and the GCPW structures). The higher insertion loss and the small difference are due to the fabrication tolerance.

The SICL-to-waveguide transition with stepped transformers measured minimum insertion loss (per transition) is 1.2 dB for K/Ka-band. The measured back-to-back structure

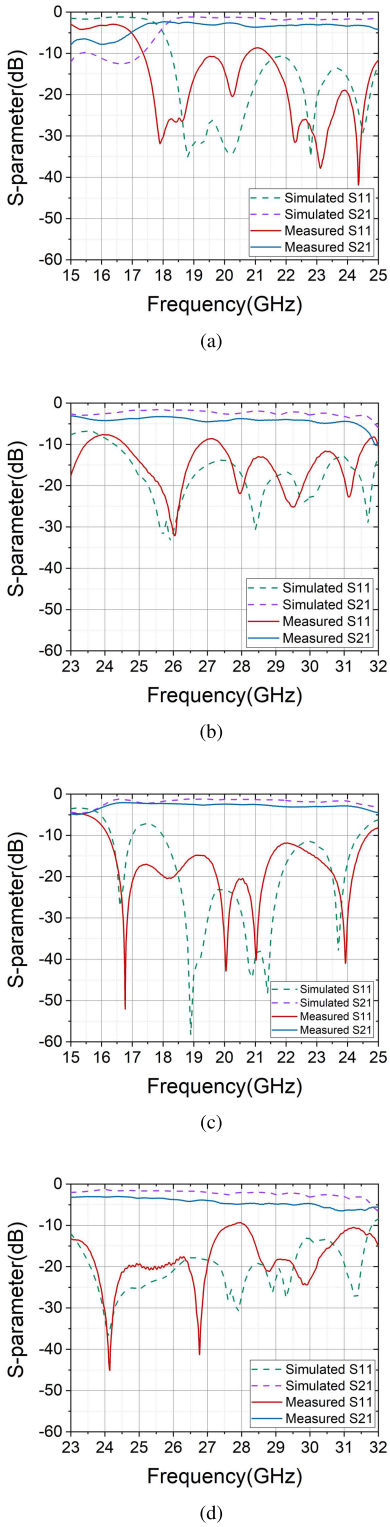

FIGURE 13. Measured results of the back-to-back waveguide transitions with stepped transformers for (a) K-band mode and (b) Ka-band mode; Measured results of the back-to-back ridge waveguide transitions for (c) K-band mode and (d) Ka-band mode.

bandwidths (return loss below 10 dB) are around 35.8% (17.4 GHz-25.0 GHz) and 25.0% (24.5 GHz-31.5 GHz) for K/Ka-band, respectively.

TABLE 1. Data of different waveguide transitions.

Ref.	Transition	IL per transition (dB)	10 dB RL (%)	Freq. band	Vertical transition	Dual band	Layers before WG transition	Size	Reconfigurable
[4]	MS-WG	<0.52	26.0	W	No	No	Single-layer	1.5λ	No
[5]	MS-WG	<0.95	11.5	Ka	Yes	No	Single-layer	1.4λ	No
[6]	MS-WG	<0.6	15.0	W	Yes	No	Single-layer	1.0λ	No
[7]	MS-WG	<1.0	20.0	V	Yes	No	Single-layer	0.9λ	No
[8]	MS-WG	<0.32	37.4	W	No	No	Single-layer	0.8λ	No
[9]	MS-WG	<0.35	37.8	W	No	No	Single-layer	0.8λ	No
[10]	SICL-WG	<0.85	21.5	W	Yes	No	Multilayer	0.8λ	No
[11]	SISL-WG	<0.34	45.7	Ka	Yes	No	Multilayer	0.8λ	No
[20]	CPW-WG	<1.2	31.5	W	Yes	No	Single-layer	1.0λ	No
[21]	SIW-WG	<1.2	40.0	K	Yes	No	Single-layer	0.9λ	No
[22]	GCPW-WG	<2.0	6.2	W	Yes	No	Single-layer	0.8λ	No
[22]	SL-WG	<2.6	33.8	W	Yes	No	Multilayer	0.7λ	No
[23]	SIW-WG	<1.0	43.0	K	Yes	No	Single-layer	0.9λ	No
[12]	GCPW-WG	<1.2 <1.0	3.0 6.7	K/Ka	Yes	Yes	Single-layer	0.7λ 1.1λ	No
[13]	SL-WG	<1.4 <1.4	8.0 15.9	K/Ka	Yes	Yes	Multilayer	0.9λ 1.0λ	No
[14]	SL-WG (Simulated)	N/A	12.3 12.9	K/Ka	Yes	Yes	Multilayer	0.6λ 1.0λ	No
TW	SICL-WG	<1.2 <1.2	35.8 25.0	K/Ka	Yes	Yes	Single-layer	0.7λ 0.9λ	Yes
TW	SICL-RWG	<1.0 <1.1	41.2 45.2	K/Ka	Yes	Yes	Single-layer	0.7λ 0.9λ	Yes

IL - Insertion Loss, RL - Return Loss, MS - Microstrip, WG - Waveguide, SL - Stripline, SICL - Substrate Integrated Coaxial Line, SISL - Substrate Integrated Suspended Line, CPW - Coplanar Waveguide, GCPW - Grounded Coplanar Waveguide, SIW - Substrate Integrated Waveguide, TW - This Work, RWG - Ridge Waveguide.

The ridge SICL-to-waveguide transition measured minimum insertion loss (per transition) is 1.0 dB and 1.1 dB for K/Ka-band, respectively. The measured back-to-back structure bandwidths (return loss below 10 dB) are around 41.2% (16.2 GHz-24.6 GHz) and 45.2% (20.2 GHz-32.0 GHz) for K/Ka-band, respectively.

Both reconfigurable SICL-to-waveguide vertical transitions with stepped transformers and ridge SICL-to-waveguide vertical transitions provided wideband performance at K/Ka-band. Table. 1 summarised and demonstrated the performance of recently published waveguide transition designs. Compared with the recent dual-band waveguide transition designs (with around 3% to 16% bandwidth), most waveguide transition designs with a single operational frequency band mode have better wideband performance and insertion loss. The comparison shows that the two presented designs have considerably better wideband performance than the recent dual-band waveguide transitions with around 25% to 45% measured bandwidth and could achieve the dual-band operation at K/Ka-band simultaneously by using the reconfigurable structure. Furthermore, the sizes (estimated dimensions of the transition designs which exclude the 50-ohm input and waveguide output) of all cited designs and these two proposed designs are listed in the table. The proposed designs have a compact footprint with 0.7λ and 0.9λ dimensions for K/Ka-band, respectively, applicable for an antenna array in MIMO beamforming applications at K/Ka-band.

IV. CONCLUSION

A K/Ka-band reconfigurable SICL-to-waveguide transition technology has been presented in this article. Two SICL-to-waveguide vertical transition designs with stepped transformers and ridge structures were designed and tested to demonstrate the design concept. Simulated and measured results had a good agreement and showed wideband performance in K/Ka-band. Furthermore, the developed SICL-to-waveguide transitions exhibit properties of reconfigurable structures and flexible functions. The presented transition technology is promising for future use in a multilayer MIMO beamforming system in satellite communication applications with all these distinctive characteristics.

ACKNOWLEDGMENT

Yifang Wei would like to acknowledge the collaboration and technical support from Tesat-Spacecom GmbH & Co. KG.

REFERENCES

[1] P. B. Saha, R. K. Dash, and D. Ghoshal, "A compact uplink-downlink band switchable wideband antenna for C-band satellite applications," in *Proc. 7th Int. Conf. Signal Process. Integr. Netw. (SPIN)*, Feb. 2020, pp. 262–266, doi: 10.1109/SPIN48934.2020.9071293.

[2] S. Cakaj and K. Malaric, "Isolation measurement between uplink and downlink antennas at low Earth orbiting satellite ground station," in *Proc. 19th Int. Conf. Appl. Electromagn. Commun.*, 2007, pp. 1–4, doi: 10.1109/ICECOM.2007.4544490.

[3] Y. Wei, C. Arnold, and J. Hong, "A K/Ka-band substrate integrated coaxial line power divider for 4-input and 16-output beamforming multi-layer feeding network," in *Proc. IEEE Asia–Pacific Microw. Conf. (APMC)*, Dec. 2020, pp. 929–931, doi: 10.1109/APMC47863.2020.9331438.

[4] M. Sarkar and A. Majumder, "A novel broadband microstrip to waveguide transition at w band with high manufacturing tolerance suitable for MMIC packaging," in *IEEE MTT-S Int. Microw. Symp. Dig.*, Nov. 2018, pp. 1–4, doi: 10.1109/IMaRC.2018.8877214.

[5] X. Dai, "An integrated millimeter-wave broadband microstrip-to-waveguide vertical transition suitable for multilayer planar circuits," *IEEE Microw. Wireless Compon. Lett.*, vol. 26, no. 11, pp. 897–899, Nov. 2016, doi: 10.1109/LMWC.2016.2614973.

[6] E. Topak, J. Hasch, and T. Zwick, "Compact topside millimeter-wave waveguide-to-microstrip transitions," *IEEE Microw. Wireless Compon. Lett.*, vol. 23, no. 12, pp. 641–643, Dec. 2013, doi: 10.1109/LMWC.2013.2284824.

[7] A. Artemenko, A. Maltsev, R. Maslennikov, A. Sevastyanov, and V. Ssorin, "Design of wideband waveguide to microstrip transition for 60 GHz frequency band," in *Proc. 41st Eur. Microw. Conf.*, 2011, pp. 838–841, doi: 10.23919/EuMC.2011.6101966.

[8] C. Wu, Y. Zhang, Y. Xu, B. Yan, and R. Xu, "Millimeter-wave waveguide-to-microstrip transition with a built-in DC/IF return path," *IEEE Trans. Microw. Theory Techn.*, vol. 69, no. 2, pp. 1295–1304, Feb. 2021, doi: 10.1109/TMTT.2020.3041257.

[9] Z. Xu, J. Xu, and C. Qian, "Novel in-line microstrip-to-waveguide transition based on E-plane probe T-junction structure," *IEEE Microw. Wireless Compon. Lett.*, vol. 31, no. 9, pp. 1051–1054, Sep. 2021, doi: 10.1109/LMWC.2021.3083281.

[10] F. Gatti, M. Bozzi, L. Perregrini, K. Wu, and R. Bosisio, "A novel substrate integrated coaxial line (SICL) for wide-band applications," in *Proc. Asia–Pacific Eur. Microw. Conf.*, Sep. 2014, pp. 70–72.

[11] Y. Chen, K. Ma, and Y. Wang, "A Ka-band substrate integrated suspended line to rectangular waveguide transition," *IEEE Microw. Wireless Compon. Lett.*, vol. 28, no. 9, pp. 744–746, Sep. 2018, doi: 10.1109/LMWC.2018.2849203.

[12] K. Erkelenz, L. P. P. B. Bohl, A. Sieganschin, and A. F. Jacob, "A compact K-/Ka-band rectangular-to-coplanar waveguide transition with integrated diplexer," *IEEE Microw. Wireless Compon. Lett.*, vol. 31, no. 6, pp. 642–645, Jun. 2021, doi: 10.1109/LMWC.2021.3064673.

[13] H. A. Diawuo and Y.-B. Jung, "Waveguide-to-stripline transition design in millimeter-wave band for 5G mobile communication," *IEEE Trans. Antennas Propag.*, vol. 66, no. 10, pp. 5586–5589, Oct. 2018, doi: 10.1109/TAP.2018.2854364.

[14] E. Arnieri, F. Greco, L. Boccia, C. Mustacchio, and G. Amendola, "Dual band topside waveguide-to-stripline transition in multilayer substrate," in *Proc. IEEE Int. Symp. Antennas Propag. USNC-URSI Radio Sci. Meeting (APS/URSI)*, Dec. 2021, pp. 691–692, doi: 10.1109/APS/URSI47566.2021.9703769.

[15] Y. Ren, K. Li, F. Wang, B. Gao, and H. Wu, "A broadband magnetic coupling microstrip to waveguide transition using complementary split ring resonators," *IEEE Access*, vol. 7, pp. 17347–17353, 2019, doi: 10.1109/ACCESS.2019.2895159.

[16] Z. Yan, Z. Ma, G. Shi, and M. Che, "A novel segmented modeling method of via including the effect of power/ground plane pair," *Int. J. Antennas Propag.*, vol. 2013, pp. 1–16, Sep. 2013, doi: 10.1155/2013/389516.

[17] Y. Hui-Wen, A. Abdelmonem, L. Ji-Fuh, and K. Zaki, "Analysis and design of microstrip-to-waveguide transitions," *IEEE Trans. Microw. Theory Techn.*, vol. 42, no. 12, pp. 2371–2380, Dec. 1994, doi: 10.1109/22.339769.

[18] J. R. Montejo-Garai, L. Marzall, and Z. Popovic, "Octave bandwidth high-performance microstrip-to-double-ridge-waveguide transition," *IEEE Microw. Wireless Compon. Lett.*, vol. 30, no. 7, pp. 637–640, Jul. 2020, doi: 10.1109/LMWC.2020.3000283.

[19] M. A. Nasr and A. A. Kishk, "Vertical coaxial-to-ridge waveguide transitions for ridge and ridge gap waveguides with 4:1 bandwidth," *IEEE Trans. Microw. Theory Techn.*, vol. 67, no. 1, pp. 86–93, Jan. 2019, doi: 10.1109/TMTT.2018.2873312.

[20] C. Wang, Y. Yao, J. Wang, X. Cheng, J. Yu, and X. Chen, "A wideband contactless CPW to *W*-band waveguide transition," *IEEE Microw. Wireless Compon. Lett.*, vol. 29, no. 11, pp. 706–709, Nov. 2019, doi: 10.1109/LMWC.2019.2945242.

[21] Y. Ding, Y. Jin, G. Zhu, Z. Zou, E. Ren, and G. Yang, "A K-band wideband low insertion loss SIW-to-waveguide transition," in *Proc. IEEE 4th Int. Conf. Electron. Technol. (ICET)*, May 2021, pp. 692–695, doi: 10.1109/ICET51757.2021.9451100.

[22] J. Jakob, R. Sammer, F. X. Rohrl, W. Bogner, and S. Zorn, "WR12 to planar transmission line transition on organic substrate," in *Proc. 49th Eur. Microw. Conf. (EuMC)*, Oct. 2019, pp. 288–291, doi: 10.23919/EuMC.2019.8910843.

[23] E. Hassan, B. Scheiner, F. Michler, M. Berggren, E. Wadbro, F. Rohrl, S. Zorn, R. Weigel, and F. Lurz, "Multilayer topology optimization of wideband SIW-to-waveguide transitions," *IEEE Trans. Microw. Theory Techn.*, vol. 68, no. 4, pp. 1326–1339, Apr. 2020, doi: 10.1109/TMTT.2019.2959759.

YIFANG WEI (Graduate Student Member, IEEE) was born in Nanjing, China, in 1994. He received the M.Sc. degree in electrical engineering from the University of Dayton, USA, in 2019. He is currently pursuing the Ph.D. degree with the Department of Electrical, Electronic and Computer Engineering, Heriot-Watt University (HWU).

His Ph.D. degree is a part of the TESLA Project H2020-MSCA-ITN, which has received funding from the European Union's Horizon 2020 Research and Innovation Program under the Marie Skłodowska-Curie Grant. His research interest includes the multilayer MIMO beamforming system based on the active phased array.

CHRISTIAN ARNOLD was born in Heilbronn, Germany, in June 1980. He received the Dipl.-Ing. (B.A.) degree from Berufsakademie Mosbach, Germany, in 2003, the Dipl.-Ing. (M.S.) degree from the Universität Stuttgart, in 2007, and the Ph.D. degree from the Universität Karlsruhe (TH), Germany, in 2017.

From August 2005 to May 2006, he studied at The University of Arizona, Tucson, Arizona. In March 2007, he joined Tesat-Spacecom GmbH & Co. KG, Backnang, Germany, as a RF Design Engineer at the Passive Microwave Products Development Group. He is currently working at Tesat-Spacecom GmbH & Co. KG, with a focus on active antennas and digital modulator products. His research interests include reconfigurable and temperature compensated filters and multiplexers for space applications. He holds several patents in these areas.

JIASHENG HONG (Fellow, IEEE) received the D.Phil. degree in engineering science from the University of Oxford, Oxford, U.K., in 1994.

He then joined the University of Birmingham, Birmingham, U.K., until 2001, when he moved up to Edinburgh, U.K., to join Heriot-Watt University, Edinburgh, where he is currently a Professor leading a team for research into advanced radio frequency (RF)/microwave device technologies. He has authored or coauthored over 200 journal articles and conference papers in this field and has published four relevant books, such as *Microstrip Filters for RF/Microwave Applications* (Wiley, first edition, 2001, and second edition, 2011), *RF and Microwave Coupled-Line Circuits* (Artech House, second edition, 2007), *Balanced Microwave Filters* (Wiley, 2018), and *Advances in Planar Filters Design* (IET, 2019).

Dr. Hong is a member of the IEEE MTT Technical Committees, the Subject Editor (Microwave) of *Electronics Letters*, and an Associate Editor of *IET Microwaves, Antennas & Propagation* and *International Journal of RF and Microwave Computer-Aided Engineering*.